Neural Drive Estimation Using the Hypothesis of Muscle Synergies and the State-Constrained Kalman Filter

Ghulam Rasool[1], Kamran Iqbal[1], Nidhal Bouaynaya[2], and Gannon White[3]

***Abstract*— We explore the hypothesis of muscle synergies to estimate the neural drive from the surface myoelectric signal. Once estimated, the neural drive can be used to control upper-extremity myoelectric prosthesis. Commonly employed pattern classification systems have certain limitations, e.g., inherent discrete nature, finite movement classes and limited degrees-of-freedom. We propose a novel framework based on the state space modeling and the hypothesis of muscle synergies. The problem is formulated in the state space framework in a novel way, where the neural drive is modeled as the hidden state of the system. A continuous stream of the neural drive (the hidden state) is estimated using a modified form of the Kalman filter. Preliminary experimental results are promising and confirm the applicability of the proposed framework.**

I. Introduction

The pattern classification algorithms have been successfully employed for upper-extremity myoelectric prosthesis control problem [1]. Such algorithms are based on the assumption that there exist distinguishable and repeatable signal patterns among different types of muscular activations [2]. Myoelectric signals are recorded from relevant upper-extremity muscles and segmentation is performed to form analysis windows. Representative features are extracted from analysis windows and a classification algorithm is trained using supervised learning. Once trained, the classification algorithm is ready to be used in real-time for movement classification [3]. Most of the classifiers reported in the literature are capable of performing classification of more than four movements with classification accuracies in the range of 90% or more [4]. However, the clinical viability of pattern classification schemes do not commensurate with the reported classification accuracies [2], [5].

The central nervous system (CNS) employs complex circuitry of spinal cord pathways to activate or relax relevant muscles in a continuous fashion to generate smooth and accurate movements. It is important to note that all quantities of interest related to such movements (i.e., the myoelectric, kinematic and kinetic signals) are continuous quantities. However, when the problem is formulated in the pattern classification domain, a discrete decision scheme results, i.e., based on the training and available myoelectric data, the classification algorithm provides a single decision about the movement (may be called "neural drive") at discrete time steps. Therefore the decision about the movement is subsequently passed on to the control mechanism at discrete time points resulting in an unnatural and jerky movement [2]. Similarly for the training of the classification algorithm, a finite set of movements is identified by the experimenter. At the most, 12 movements are reported in the literature [4]. The classification algorithm will be able to classify only movements for which it has been trained. Therefore, the prosthesis will be able to perform only a limited set of movements for which the classification algorithm was trained. Number of classes can be increased at the expense of a complex and computationally expensive classifier. However, the limitation of real-time decision making limits the applicability of such an approach. Furthermore, a single decision from the pattern classification system activates only a single degree-of-freedom (DOF) movement, i.e., the scheme implements a sequential control rather than simultaneously activating multiple DOFs. This is in contrast to human motor control where multiple DOFs are simultaneously activated as a routine [2].

How the CNS generates, coordinates, controls and executes voluntary movements has been a long-standing question. It is hypothesized that the CNS may employ certain building blocks to generate complex movements, called the "Muscle Synergies". Specifically, muscle synergies have been proposed as discrete elements which can be combined to produce original motor solutions [6]. By definition, muscle synergies are *fixed relative levels of activation of different muscles* [7]. We propose to use the hypothesis of muscle synergies to estimate the neural drive in upper-extremity voluntary movements.

This paper presents preliminary results of our ongoing research, focused on the investigation of the hypothesis of muscle synergies and state space modeling for estimation of neural drive using the surface myoelectric signal.

II. State Space Model of the Problem

We propose to model the "neural drive" as the unknown hidden state in our state space scheme. Systems dynamics are modeled using the *random walk* model, while the hypothesis of muscle synergies is used to find the system observation model. Subsequently, we employed a modified form of the Kalman filter to estimate the hidden state, i.e., the neural drive. A non-negativity constraint was forced on the estimation algorithm due to physiological reasons, i.e., the neural drive is a nonnegative quantity.

[1] Systems Engineering Department, University of Arkansas at Little Rock, Little Rock, AR-72204, USA. gxrasool, kxiqbal@ualr.edu.

[2] Electrical and Computer Engineering Department, Rowan University, Glassboro, NJ-08028, USA.

[3] Department of Health, Human Performance, and Sport Management at University of Arkansas at Little Rock, Little Rock, AR-72204, USA. gawhite@ualr.edu

A. State Space Model

For a discrete linear system, we have

$$\mathbf{x}(k+1) = F\mathbf{x}(k) + G\mathbf{u}(k) + \mathbf{w}_1(k), \quad (1)$$

$$\mathbf{y}(k) = H\mathbf{x}(k) + \mathbf{w}_2(k), \quad (2)$$

where, F, G and H are known matrices of appropriate dimensions and represent linear system dynamics, input-state coupling, and output-state coupling respectively, $\mathbf{x}(k)$ is the state, $\mathbf{u}(k)$ is the input, $\mathbf{y}(k)$ is the output, $\mathbf{w_1}(k)$, and $\mathbf{w_2}(k)$ are system and observation noise respectively.

1) System Dynamics Model: The system dynamics model captures the future evolution of the state. We assume no *a priori* knowledge about evolution of system state and therefore propose a random walk model. From (1), we get

$$\mathbf{x}(k+1) = \mathbf{x}(k) + \mathbf{w}_1(k). \quad (3)$$

2) System Observation Model: The observation model is derived from the hypothesis of muscle synergies. The muscle synergy matrix W is a $m \times n$ matrix whose columns are the muscle synergies with m number of muscles and n number of synergies. By definition, we have

$$\mathbf{v}(k) = W \times \mathbf{h}(k), \quad (4)$$

where the vector $\mathbf{v}(k)$ specifies activation levels of all m muscles, $\mathbf{h}(k)$ is an n-element neural drive vector at time k and '$\times$' represents the matrix product. The muscle synergy matrix defines a linear mapping between the state (neural drive) and the output (myoelectric data). The non-negative matrix factorization (NMF) algorithm is used to estimate the muscle synergy matrix W from the processed surface myoelectric data [8]. Once the muscle synergy matrix W is known, we use it as an observation matrix in our state space representation. From (2), we get

$$\mathbf{y}(k) = W\mathbf{x}(k) + \mathbf{w}_2(k). \quad (5)$$

B. The Kalman Filter

Kalman filter is the minimum mean-square estimator for linear systems with additive Gaussian noise, where state estimate is found by propagating the mean and variance of the state [9]. For the problem under investigation, we propose to model system noise $\mathbf{w}_1(k)$ and observation noise $\mathbf{w}_2(k)$ with a Gaussian process. This assumption seems reasonable as the evolution of the system state and observations over time are centered around a mean value. Some relevant assumptions about the system noise $\mathbf{w}_1(k)$ and observation noise $\mathbf{w}_2(k)$ are,

$$\begin{aligned} \mathbf{w}_1(k) &\sim \mathcal{N}(0, Q_k), \\ \mathbf{w}_2(k) &\sim \mathcal{N}(0, R_k), \\ E[\mathbf{w}_1(k)\mathbf{w}_1(j)] &= Q_k\delta_{kj}, \\ E[\mathbf{w}_2(k)\mathbf{w}_2(j)] &= R_k\delta_{kj}, \\ E[\mathbf{w}_1(k)\mathbf{w}_2(j)] &= 0, \end{aligned} \quad (6)$$

where δ is the Kronecker delta function with $\delta_{kj} = 1$ for $k = j$ and zero otherwise.

The Kalman filter performs recursive estimation of the unknown state and is there much suited for real-time applications, such as the neural drive estimation. Kalman filter recursion can be described by the prediction and the filtering part [9]. Using system dynamics and observation models given in (3) and (5), we have

[Prediction]

$$\begin{aligned} &\mathbf{x}(k|k-1) = \mathbf{x}(k-1|k-1), \\ &V(k|k-1) = V(k-1|k-1) + Q_k. \end{aligned} \quad (7)$$

[Filtering]

$$\begin{aligned} &K(k) = V(k|k-1)W_k^T[W_kV(k|k-1)W_k^T + R_k]^{-1}, \\ &\mathbf{x}(k|k) = \mathbf{x}(k|k-1) + K_k[\mathbf{y}(k) - W(k)\mathbf{x}(k|k-1)], \\ &V(k|k) = [I - K(k)W(k)]V(k|k-1), \end{aligned} \quad (8)$$

where $K(k)$ is the Kalman gain and $V(k|.)$ is the state covariance matrix. Given initial conditions, i.e., $\mathbf{x}(0|0)$ and $\mathbf{V}(0|0)$, the Kalman filter recursively estimates the state vector.

C. The State-Constrained Kalman Filter

In its original form the Kalman filter does not incorporate any prior available information about the unknown state into its estimate. However, the filter can be modified to do so [10]. In our proposed framework, there is a physiological constraint of non-negativity on the state vector $\mathbf{x}(k)$, i.e., the neural drive cannot be a negative quantity. Various approaches have been adopted to include constraints into the state estimation problem, i.e., model reduction, perfect measurement, probability distribution function truncation and the estimate projection [10]. We used the estimate projection approach and projected the estimated state vector onto a non-negative sub-space. Given the state estimate $\hat{\mathbf{x}}$, we project it onto a non-negative space to get $\tilde{\mathbf{x}}$.

$$\tilde{\mathbf{x}} = \underset{\tilde{\mathbf{x}}}{\operatorname{argmin}} (\tilde{\mathbf{x}} - \hat{\mathbf{x}})^T(\tilde{\mathbf{x}} - \hat{\mathbf{x}}) \text{ such that } \tilde{\mathbf{x}} \succeq \mathbf{0}, \quad (9)$$

where $\succeq$ implies element-wise inequality. The problem in (9) is a convex optimization problem and standard optimization routines can be used to find the optimal solution.

III. Methods

The study received approval from the Institutional Review Board (IRB) of the University of Arkansas at Little Rock. We identified two distinct groups of movements for our data collection experiment, i.e., movements performed by the hand, and by the wrist. Hand movements included three types of grasps, i.e., lateral grasp, cylindrical grasp, and tripod grasp, and two other movements which included hand open and index finger point [4]. While the wrist movements included wrist pronation and supination, ulnar and radial deviation, and wrist flexion and extension. Keeping in view the selected set of movements, we identified physiologically relevant muscles for myoelectric data recording which included muscle *pronator teres* (PT), muscle *flexor carpi radialis* (FCR), muscle *palmaris longus* (PL), muscle *flexor carpi ulnaris* (FCU), muscle *brachioradialis* (BR), muscle

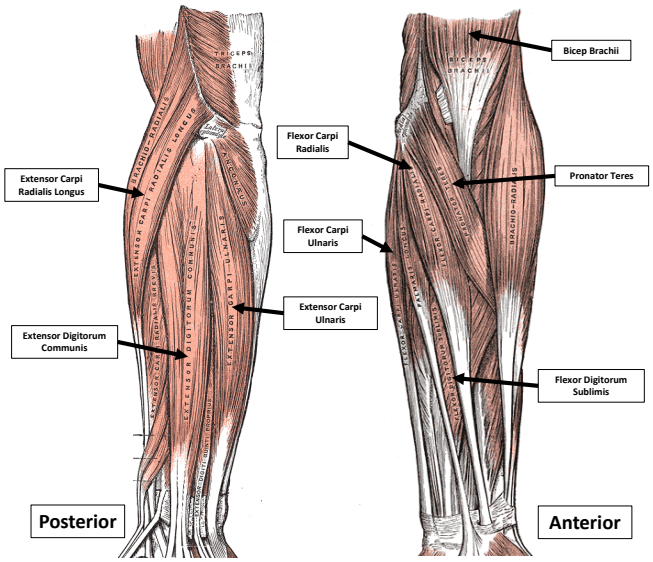

Fig. 1. Placement of electrodes around the forearm on anterior and posterior sides.

extensor carpi radialis (ECR) muscle *extensor digitorum communis* (EDC), and muscle *extensor carpi ulnaris* (ECU). Fig. 1 shows locations of these muscles in the forearm from both anterior and posterior sides.

A. Myoelectric Data Collection

A Noraxon (Noraxon U.S.A. Inc, Scottsdale, Arizona) TeleMyo Direct Transmission System (DTS) was used to record the myoelectric data. Eight wireless probes were used to record and transmit data at a sampling rate of 1500 Hz. Eight disposable, self-adhesive silver/silver chloride (Ag/AgCl) snap electrodes with two circular conductive areas is of 1 cm each and an inter-electrode distance of 2 cm were used. Muscle identification was performed using palpation and electrodes were placed over the belly of the selected muscle. Quality of myoelectric signals was monitored to ensure correct muscle identification. Myoelectric signals were recorded using the Noraxon software (MyoResearch XP) and stored on the hard disk for later processing. All offline data processing was done in Matlab (Version 7.12.0.635, R2011a, The MathWorks, Natick, MA).

B. Experimental Protocol

Before start of the data collection experiment, the participant was sitting comfortably on a chair. Initial/rest position of the arm was defined as: the dorsopalmar axis pointing inside parallel to coronal plane (palm facing to the medial side of the body with forearm parallel to the ground), elbow flexed at 90^o and arm abducted 10^o. Forearm was supported at two places, i.e., under the styloid process of the ulna and the distal end of the humerus (the elbow joint). A graphical user interface (GUI) based software was used to provide visual and auditory clues to participants for guiding through the data collection process. A single trial consisted of one repetition of each movement for a duration of 5 seconds. There was a short break of 4 seconds between consecutive movements.

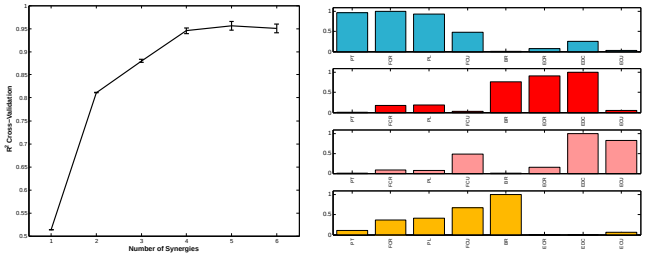

(a) Cross-validation results. (b) Muscle synergies.

Fig. 2. (a) The coefficient of determination R^2 for cross-validation in order to select adequate number of muscle synergies. Four muscle synergies were sufficient to explain more than 90% variability in the data. (b) A set of four representative muscle synergies extracted from the myoelectric data.

Between every two trials, there was an additional break, duration of which was left at the discretion of the participant. Participants were instructed to start the movement from defined initial (rest) position, stay in the prescribed posture (shown in the GUI) and then return back to initial position upon visual and auditory clue.

C. Myoelectric Data Processing

Root mean square (RMS) of the reocrded myoelectric data was calculated for each 250 ms window. This value represented activation level of all muscles under investigation, i.e., $\mathbf{v}(k)$ in (4). The matrix V was formed by placing $\mathbf{v}(k)$ as columns of V for $k = 1, \ldots, K$, where K is the total number of windows. Once matrix V is formed, the NMF algorithm was used to estimate the muscle synergy matrix W [8].

IV. Experimental Results

In this section we present preliminary experimental results. First we present results related to extraction of muscle synergies and later for the state-constrained Kalman filter.

A. Extraction of Muscle Synergies

We used the NMF algorithm and a five-fold cross-validation scheme for extraction of muscle synergies from the myoelectric data. Cross-validation was performed using modified NMF algorithm, where the extracted muscle synergies matrix W is supplied to the NMF algorithm with new data V_{new} (not used to extract muscle synergies) and an estimate of H_{est} is found. The newly estimated matrix H_{est} is used with already extracted muscle synergy matrix W to find the estimated data matrix V_{est} using the relation $V_{est} = W \times H_{est}$. For reporting the cross-validation results we use the coefficient of determination R^2,

$$R^2 = 1 - \frac{\sum\limits_i (y_i - \hat{y}_i)^2}{\sum\limits_i (y_i - \bar{y})^2}, \tag{10}$$

where $\hat{y}_i$ is the estimate of y_i and $\bar{y} = \frac{1}{n}\sum\limits_i y_i$. It is evident from Fig. 2(a) that four muscle synergies explain more than 90% data variability. Fig. 2(b) presents four extracted muscle synergies.

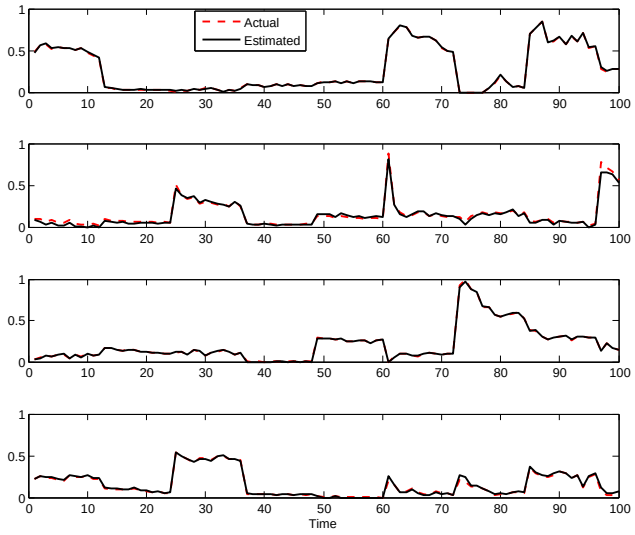

Fig. 3. Neural drive estimation using the state-constrained Kalman filter. The ground truth and estimated neural drive are normalized.

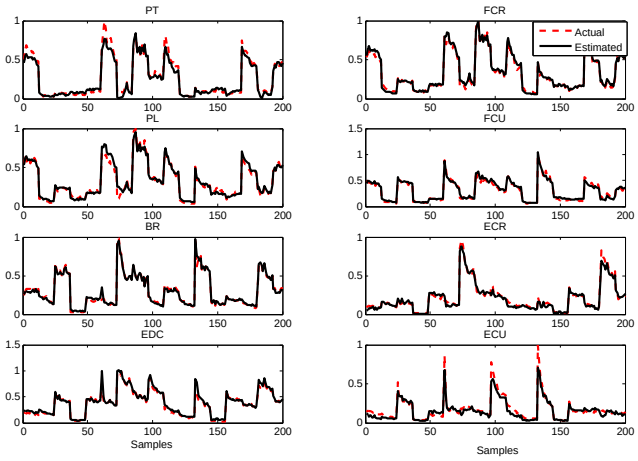

Fig. 4. Reconstruction of normalized muscle activations using the neural drive estimate from the state-constrained Kalman filter.

B. The State-Constrained Kalman Filter

The state-constrained Kalman filter was employed to estimate the hidden state, i.e., the neural drive. The NMF algorithm was used to extract muscle synergies matrix W and the neural drive matrix H from the processed myoelectric data, the matrix V. The synergy matrix W was used as the observation matrix in (5), while the neural drive matrix H was stored as the *ground truth*. As we have four muscle synergies, the state vector consists of four variables, i.e., one coefficient for each of the four synergies. Processed myoelectric data was provided to the state-constrained Kalman filter for estimation of the state. In Fig. 3, we provide estimated neural drive for 100 time-points (each time point represents a 250 ms window) and the ground truth. The state vector was reconstructed with $R^2 = 97.17\%$. After estimating the neural drive using the state-constrained Kalman filter, we estimate muscle activations also, using the estimated neural drive and muscle synergy matrix. In Fig. 4, we present reconstruction of normalized activations of all eight muscles for 200 time-points with $R^2 = 97.07\%$.

It is evident from Fig. 3 and Fig. 4 that the state-constrained Kalman filter has successfully been able to estimate the neural drive and reconstruct muscle activations. However, the whole data processing was done in off-line mode. The next goal of the research is to perform the state tracking (i.e., neural drive estimation) in real time.

V. Conclusion

We proposed a novel framework for estimation of neural drive from the surface myoelectric signal in the case of upper-extremity movements. The whole problem was modeled in the state space framework with the system dynamics given by the random walk and observation dynamics by the hypothesis of muscle synergies. Modified form of the Kalman filter with non-negativity constraint was successfully employed to find an estimate of the neural drive. Preliminary results were also presented which confirmed the applicability of the proposed scheme.

References

[1] E. Scheme and K. Englehart, "Electromyogram pattern recognition for control of powered upper-limb prostheses: State of the art and challenges for clinical use," *The Journal of Rehabilitation Research and Development*, vol. 48, no. 6, p. 643, 2011.

[2] N. Jiang, S. Dosen, K.-R. Muller, and D. Farina, "Myoelectric control of artificial limbs - is there a need to change focus?" *IEEE Signal Processing Magazine*, vol. 29, no. 5, pp. 152 –150, Sep. 2012.

[3] S. Micera, J. Carpaneto, and S. Raspopovic, "Control of hand prostheses using peripheral information," *Biomedical Engineering, IEEE Reviews in*, vol. 3, pp. 48 –68, 2010.

[4] B. Peerdeman, D. Boere, H. Witteveen, R. H. in 't Veld, H. Hermens, S. Stramigioli, H. Rietman, P. Veltink, and S. Misra, "Myoelectric forearm prostheses: state of the art from a user-centered perspective," *Journal of rehabilitation research and development*, vol. 48, no. 6, pp. 719–737, 2011.

[5] B. Lock, K. Englehart, and B. Hudgins, "Real-time myoelectric control in a virtual environment to relate usability vs. accuracy," in *Proceedings of the 2005 MyoElectric Controls/Powered Prosthetics Symposium*. Fredericton, New Brunswick, Canada, August 17-19, 2005.

[6] E. Bizzi, V. Cheung, A. d'Avella, P. Saltiel, and M. Tresch, "Combining modules for movement," *Brain Research Reviews*, vol. 57, no. 1, pp. 125–133, Jan. 2008.

[7] J. Roh, W. Z. Rymer, and R. F. Beer, "Robustness of muscle synergies underlying three-dimensional force generation at the hand in healthy humans," *Journal of neurophysiology*, vol. 107, no. 8, pp. 2123–2142, Apr. 2012.

[8] L. H. Ting and S. A. Chvatal, "Decomposing muscle activity in motor tasks," in *Motor Control: Theories, Experiments, and Applications*. Oxford University Press, Dec. 2010.

[9] D. Simon, *Optimal State Estimation: Kalman, H Infinity, and Nonlinear Approaches*, 1st ed. Wiley-Interscience, Jun. 2006.

[10] ——, "Kalman filtering with state constraints: a survey of linear and nonlinear algorithms," *IET Control Theory Applications*, vol. 4, no. 8, pp. 1303–1318, Aug. 2010.